Available online at www.sciencedirect.com

SciVerse ScienceDirect

Scripta Materialia 68 (2013) 404–407

Scripta MATERIALIA

www.elsevier.com/locate/scriptamat

Fracture behavior of hydroxyapatite nanofibers in dental enamel under micropillar compression

Ezgi D. Yilmaz,[a] Sabine Bechtle,[a] Hüseyin Özcoban,[a] Andreas Schreyer[b] and Gerold A. Schneider[a,*]

[a] *Institute of Advanced Ceramics, Hamburg University of Technology, Hamburg, Germany*
[b] *Institute of Materials Research, Helmholtz-Zentrum Geesthacht, Geesthacht, Germany*

Received 3 September 2012; revised 30 October 2012; accepted 4 November 2012
Available online 10 November 2012

Understanding the structure–property relations of load-bearing natural materials can provide design strategies for the generation of bio-inspired materials showing enhanced mechanical properties. Dental enamel is a highly damage-tolerant biological nanocomposite having a high mineral content. Its hierarchical structure consists of hydroxyapatite nanofibers enveloped by proteins on the smallest length scale. In this work, we show the fracture behavior of nanofibers in enamel by conducting micropillar compression tests. The evaluation and the result of the mechanical properties are discussed.

Keywords: Dental enamel; Hydroxyapatite; Biological materials; Micro-compression

Dental enamel is a naturally occurring hierarchically structured biocomposite which is the hardest substance in the human body. It is able to continue its function through millions of chewing cycles where the contact stresses can reach up to 2.5 GPa [1], despite the fact that it contains inherently crack-like defects [2]. Enamel is a highly mineralized tissue, up to ~85 vol.% [3] of which consists of nanoscaled hydroxyapatite (HAP) fibers surrounded by organic molecules arranged into parallel aligned rod-like structures separated by protein-rich sheaths, as shown in Figure 1. The enamel rods starting at the enamel–dentin junction have a wavy outline which is organized into groups with different orientations crossing each other to form the so-called decussation pattern [4–6]. Studies of the macroscopic fracture behavior of enamel [2,5,7,8] have found that this morphological feature is responsible for its high damage tolerance by providing resistance to crack propagation, which is considered as a natural adaptation to the stresses generated during mastication [2,9]. On the other hand, the fracture behavior of its nanoscale features alone has not been extensively investigated; what studies there have been have focused mostly on nanoindentation, assessing the material properties under complex multi-axial stress states and constrained conditions due to the surrounding bulk material.

However, new mechanical testing techniques have emerged in recent years which enable uniaxial loading of focused ion beam (FIB) milled micron-and nanoscaled samples and also visual inspection of the as-deformed samples to analyze their failure modes, which is not possible by nanoindentation. For example, micropillar compression experiments have become an important tool for studying local mechanical properties of small volumes so as to understand the fundamentals of size-dependent deformation and the damage behavior of complex multi-phase, multi-structured systems and thin films, which is of importance for the reliability of many miniaturized instruments and nanosytems [10–13]. In many metallic systems it has been shown that the flow stresses scale up as the micropillar diameter decreases; this is mostly explained by the dislocation starved conditions that prevail in small volumes [10–15]. In addition to this extrinsic size effect, intrinsic (microstructural) effects, such as dislocation density, grain size and precipitation size, have also been found to contribute to the strengthening in micropillars [10]. A few researchers have also applied micromechanical tests to biological materials [4,5,16–21], which are believed to exhibit a heterogeneous behavior on different length scales due to their unique hierarchical microstructures [22]. For example, Bechtle et al. [4] examined the

* Corresponding author. Tel.: +49 40 42878 3037; fax: +49 40 42878 2647; e-mail: g.schneider@tuhh.de

1359-6462/$ - see front matter © 2012 Acta Materialia Inc. Published by Elsevier Ltd. All rights reserved.
http://dx.doi.org/10.1016/j.scriptamat.2012.11.007

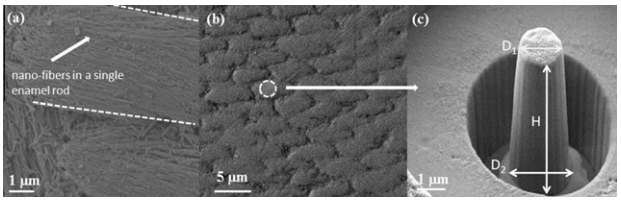

Figure 1. (a) SEM image of HAP nanofibers (20–50 nm in wide), which are believed to be surrounded by a thin (1–2 nm) organic layer [20], are bundled together to form cylindrically shaped enamel rods which are around 5 μm in diameter. (b) SEM image of the rod cross-sections separated by protein-rich sheaths shows the FIB cut placement for μ-pillar fabrication. (b) A representative μ-compression test sample with tapered pillar geometry which consists of HAP nanofibers parallel to the pillar long axis.

bending response of different sized enamel samples on the micron scale and found an almost twofold drop in flexural strength and modulus accompanied by a switch from brittle to more damage-tolerant mechanical behavior with each decreasing hierarchical level (increasing sample size). This trend was attributed to an intrinsic effect of the protein content, which varies at each hierarchical level. Considering the fact that teeth operate essentially under compressive stresses, in this study we conduct micropillar compression tests on dental enamel to study the fracture behavior of nanosized HAP fibers.

Bovine enamel was investigated in this study as it exhibits a very similar microstructure and composition to human enamel [5]. For details on teeth storage and sample preparation for the FIB milling process, see Ref. [17]. Figure 1b displays enamel rod cross-sections in which the nanofibers are oriented perpendicularly or nearly perpendicularly to the outer surface. We attempted to fabricate cylinder-shaped columns within an enamel rod by the FIB milling technique for micro-compression testing proposed by Uchic and Dimiduk [11], using a CrossBeam Zeiss Auriga Canion FIB system. First, rough cutting with a Ga-ion beam current of 2 nA at 30 kV was used to mill a trench perpendicular to the polished surface with a diameter of ~20 μm around the pillar. This ensures that the flat-ended indenter tip loads only the pillar itself and not onto the surrounding material. This was followed by a fine milling procedure with a decreased beam current of 200 pA to obtain an accurate geometry and smooth sidewalls. However, it is almost impossible to prevent tapering of the pillar sidewalls by the annular cutting method [11], and this results in a non-uniform diameter size throughout the length of the pillar. This can be quantified by the taper angle α (typical α values reported in the literature are between 1° and 7° [12,14,23–25], which is calculated by arctan $((D_2-D_1)/(2 \times H))$, where D_1 and D_2 are the top and bottom diameters of the pillar respectively, and H is the pillar length (Fig. 1c). The geometrical data's of the μ-pillar specimens are given in Table 1.

As-prepared μ-pillars were loaded using an Agilent Nano Indenter G200 system with a diamond flat-ended punch with a diameter of 10 μm. The nanoindentation tests were set to a single load/unload cycle to a specified compression depth (Table 1), with a loading segment imposing a constant strain rate of 0.05 s^{-1}. Automatic correction for the frame compliance and thermal drift were implemented on the load–displacement data. Figure 2a shows the load–displacement curves corresponding to the four μ-pillars. All the curves can be characterized by an initial linear-elastic deformation followed by sudden fracture events, resulting finally in large displacement bursts. It should be noted that the non-linearity at the beginning of the load–displacement curve and the low pillar stiffness can result from the initial settling of the indenter on the sample surface, which is not perfectly flat [13,14,25].

Evaluation of the stress–strain curves from the μ-compression test samples is complicated due to the tapered pillar geometry and the sink-in of the pillar into the underlying base material as a result of the fixed pillar end, which was estimated to be 15–20% of the total displacement in a numerical study for anisotropic single crystals [25], and observed by visual inspection during in situ scanning electron microscopy (SEM) measurement of Si μ-pillars [26]. Therefore, an analytical approach for the correction of the base displacement was used in most of the μ-compression studies [12,25,26], which is based on the solution of a perfectly rigid cylindrical punch pressed into an elastic half-space derived by Sneddon [27]. This correction procedure requires knowledge of the elastic modulus and Possion's ratio of the underlying base material. However, there is a discrepancy in the elastic modulus values reported for enamel in the literature, depending on the anisotropy, hierarchy, testing conditions and parameters [1,4,5,20,28–32]. Varying the used elastic modulus value of the bulk enamel from 30 to 80 GPa in the correction can alter the computed elastic modulus of the pillar by up to 30%. Therefore, we applied the formula for the normalized stress–strain calculation proposed by Han et al. [21], which avoids the pre-requirement of the elastic modulus value of the bulk material for the correction of the base displacement. Han et al. also employ Sneddon's solution for the correction of the base compliance by applying it in the stress calculation generated within the pillar and

Table 1. Dimensions and mechanical properties of enamel μ-pillars tested in this study compared with data from the literature.

Pillar No.	D_1 (μm)	D_2 (μm)	H (μm)	Aspect ratio $H/((D_1+D_2)/2)$	Taper angle α (°)	Compression depth target (nm)	Fracture stress, σ_F (MPa)	Fracture strain, ε_F (%)	Elastic modulus, E (GPa)
1	2.22	3.16	5.86	2.18	4.62	300	927	4.5	32
2	2.12	3.34	4.74	1.59	4.37	200	888	2.9	40
3	2.13	2.62	4.23	1.78	3.3	200	749	3	40
4	2.61	3.34	6.69	2.45	5.25	500	891	2.8	48
[21]	1	1.24	3	2.7	2.25	120	~1100	2–3	~50